Rev. Mexicana Astron. Astrof., 15, 125-132 (1987)

LOW DENSITY ENVELOPES OF SOUTHERN H II REGIONS

I.N. Azcárate[1], J.C. Cersosimo[1], and F.R. Colomb[1]

Instituto Argentino de Radioastronomía
Argentina

Received 1987 August 10

RESUMEN

Se han estudiado las envolturas de gas ionizado de baja densidad asociadas a algunas regiones H II, mediante observaciones de la línea de recombinación de H166α y el continuo en 1.4 GHz. Se obtuvieron de las mismas algunos parámetros físicos. Las regiones H II observadas son: RCW 49, G 338.4+0.0, G 331.5−0.1, W 31, RCW 122 y RCW 38. Se observa en estas regiones la misma estructura ya observada en otras regiones H II, consistente de una pequeña región compacta y una envoltura extendida de gas de baja densidad.

ABSTRACT

Extended and low density ionized gas envelopes associated to some H II regions, have been studied in the H166α recombination line and the continuum at 1.4 GHz. From these observations, values of some physical parameter have been obtained. The observed H II regions are the following: RCW 49, G 338.4+0.0, G 331.5 − 0.1, W 31, RCW 122 and RCW 38. In these regions we have observed a structure similar to other H II regions which consists of a small compact H II region with an extended low density envelope.

Key words: NEBULAE-H II REGIONS – RADIO CONTINUUM – RADIO LINES-RECOMBINATION

I. INTRODUCTION

In this paper, we studied the low density ionized envelopes associated to the six nebulae mentioned in the abstract.

a) *RCW 49*

This region has been observed previously in the H109α line (Wilson *et al.* 1970) with H76α line (Mc Gee and Newton 1981), and in molecular lines like H_2CO in absorption (Whiteoak and Gardner 1974), CO in emission (Gillespie *et al.* 1977), OH (Caswell and Robinson 1974). The CO emission velocity is 16 km s^{-1}, a remarkable difference with respect to the H_2CO absorption and OH velocities of −14.1 km s^{-1} and −13 km s^{-1}, respectively (throughout this paper, all velocities are referred to the LSR). There is some obscuration in front of RCW 49 and a 10μ source in the same direction (Gillespie *et al.* 1977). Then, the velocity differences could indicate that CO is associated with the foreground dust rather than with RCW 49. Recombination line velocities are 1 km s^{-1}.

b) *G 338.4+0.0*

This region, which has been scarcely studied, has been observed previously in the H109α line (Wilson *et al.* 1970), and molecular lines such as H_2CO in absorption (Whiteoak and Gardner 1974), OH (Caswell and Robinson 1974). The recombination line velocity is −36.9 km s^{-1}. The H_2CO absorption velocity is −29.1 km s^{-1}. The OH absorption velocity is −34 km s^{-1}.

c) *G 331.5−0.1*

This region has been previously observed in the recombination lines of H109α (Wilson *et al.* 1970), H76α (Mc Gee and Newton 1981) and H90α (Mc Gee, Newton, and Batchelor 1975), and in molecular lines such as H_2CO (Whiteoak and Gardner 1974), OH (Caswell and Robinson 1974), and HCN (Whiteoak and Gardner 1978). Recombination line velocities agree rather well with those of the molecular lines, ranging from −88 to −93 km s^{-1}.

d) *W 31*

This region has been studied in H109α (Wilson *et al.* 1970), H76α (Mc Gee and Newton 1981) and in the molecular lines of H_2CO (Whiteoak and Gardner 1974) and HCN (Whiteoak and Gardner 1978). There is good agreement between velocities obtained from recombination line observations and molecular lines, ranging from 10 to 14 km s^{-1}.

1. Member of the Carrera del Investigador Científico y Tecnológico del Consejo Nacional de Investigaciones Científicas y Técnicas, Argentina.

e) *RCW 122*

This region, centered at $l = 348^\circ.7$, $b = -1^\circ.0$, was observed previously in lines of H109α (Wilson *et al.* 1970), H76α (Mc Gee and Newton 1981), and in the molecular lines like H_2CO (Whiteoak and Gardner 1974), OH (Caswell and Robinson 1974), and HCN (Whiteoak and Gardner 1978). Recombination line velocities which lie between −12 to −13 km s^{-1} agree rather well with those of the molecular lines.

f) *RCW 38*

This region has been studied in H109α (Wilson *et al.* 1970), H76α (Mc Gee and Newton 1981), H90α (Mc Gee *et al.* 1975), H159α (Cersosimo 1985) and in the molecular lines H_2CO (Whiteoak and Gardner 1974), CO (Gillespie *et al.* 1977), HCN (Whiteoak and Gardner 1978), and OH (Caswell and Robinson 1974). Recombination line and molecular line velocities range from 1 to 4 km s^{-1}.

In the next section we will describe observations of the six H II regions in the H166α line and in the 1.4 GHz continuum.

II. OBSERVATIONS

a) *The Line*

The observations were made with the 30-meter antenna of the Instituto Argentino de Radioastronomía. The noise temperature of the system was about 85 K for a cold sky background and the antenna beam was 34 arcmin at 1420 MHz. The frequency-switching technique was used for the observations. A filter bank of 112 filters of 10 kHz width gave a velocity resolution of 2 km s^{-1}.

For most of the regions, eight or nine positions were observed at a separation of $0^\circ.5$ (except RCW 38, observed at only one position). The total integration time was about 3–4 hours for each position. The "rms" noise was $\sim$ 0.02 K.

Finally, the profiles were obtained by removing in most cases, only a second order polynomial. In a few cases, the use of a third order polynomial was necessary.

b) *The Continuum*

The continuum observations of all the regions were made by making several right ascension scans spaced $0^\circ.5$ in declination. The continuum receiver covered a bandwidth of 40 MHz centered at 1420 MHz.

For the elimination of galactic neutral hydrogen, a filter of 2 MHz bandwidth centered at 1420.4057 MHz was used. The receiver was operated in the Dicke switching mode for all the continuum observations. The velocity of the right ascension scans was $0^\circ.5$ per minute.

III. RESULTS

a) *RCW 49*

Some H166α profiles of the extended region are shown in Figure 1. The central velocities of the profiles are $\sim$ 1.5 km s^{-1}, with a FWHM of $\sim$ 35 km s^{-1}.

The continuum map at 1420 MHz of the extended region is shown in Figure 2. The positions where the H166α line was observed are indicated by crosses. The average electron temperature is $\sim$ 5650 K. The flux density in the continuum corresponding to the extended region of 120′ of angular diameter is $\sim$ 1000 Jy (flux units). By using the simplified spherical model of Schraml and Mezger (1969), we obtain values of $N_e \sim 4.5$ cm^{-3} and emission measure (E.M.) $\sim 6.12 \times 10^3$ pc cm^{-6}

Results for N_e and E.M. obtained from higher frequency recombination lines (Wilson *et al.* 1970; Mc Gee and Newton 1981) show values between 2 and 3

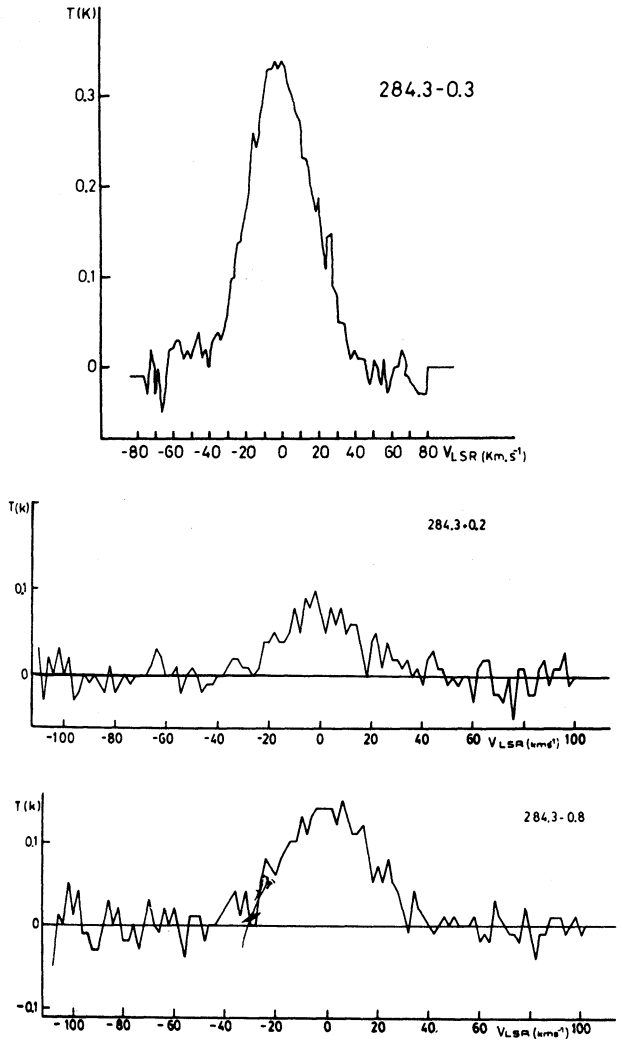

Fig. 1. Some profiles of the H166α line in the RCW 49 region.

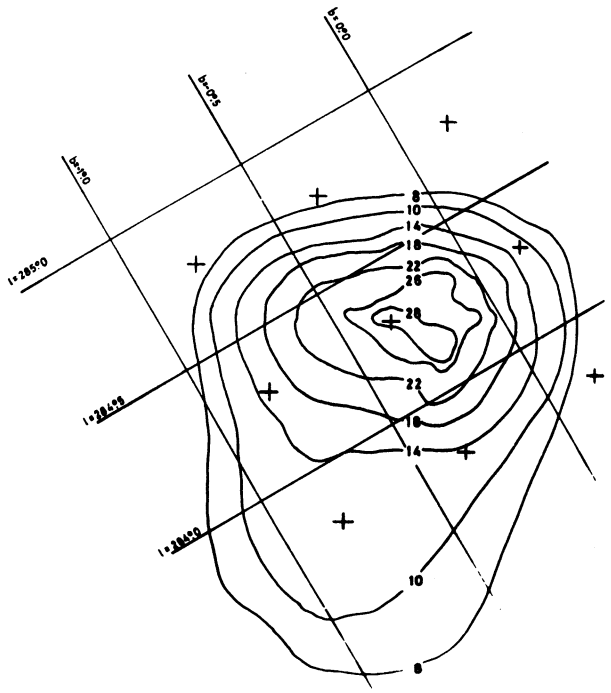

Fig. 2. Continuum map at 1420 MHz of the extended region associated with RCW 49. The crosses indicate the positions where the line observations were made.

orders of magnitude greater than our H166α results (see Table 1). That happens because at the frequency of the H166α line and with our relatively large antenna beam, the observations are more sensitive to the extended and diffuse parts of the nebula, while the compact and higher emission measure regions near the center of the nebula become optically thick at 1.4 GHz, suffering thus greater beam dilution.

b) *G 338.4+ 0.0*

Some of the H166α profiles obtained in the extended region are shown in Figure 3. The central velocities of the profiles are ~ -40 km s^{-1}. The FWHM of most of them is ~ 35 km s^{-1}.

We show the 1420 MHz continuum map in Figure 4. The positions where the line was observed are shown by X marks. The continuum integrated flux density of the extended region of 105′ of angular diameter is ~ 1120 Jy. The average electron temperature obtained is ~ 6200 K. By using the same spherical model as that adopted for the other regions, we obtained a mean value for the electron density $N_e \sim 2.88$ cm^{-3} and for the emission measure $\sim 8.44 \times 10^3$ pc cm^{-6}. The values obtained from higher frequency recombination line observatios (Wilson *et al.* 1970), are 2 or 3 orders of magnitude greater than the H166α values (see Table 1). The same explanation given for RCW 49 is also valid here.

TABLA 1

VALUES OF ELECTRON DENSITY, EMISSION MEASURE AND TEMPERATURE FOR THE H II REGIONS STUDIED IN THIS PAPER[a]

Region	Parameter	H166α	H109α	H76α
RCW 49	T_e (K)	5650	6800	8520
	E.M. (pc cm^{-6})	6.12 × 10^3	6.6 × 10^5	7 × 10^5
	N_e (cm^{-3})	4.46	218	265
G 338.4 + 0.0	T_e (K)	6194	4900	....
	E.M. (pc cm^{-6})	8.44 × 10^3	1 × 10^5	....
	N_e (cm^{-3})	7.88	1 × 10^2	....
G331.5 – 0.1	T_e (K)	5750	5200	6285
	E.M. (pc cm^{-6})	3.58 × 10^3	5.8 × 10^5	5.1 × 10^5
	N_e (cm^{-3})	2.76	232	275
W 31	T_e (K)	5600	4700	5939
	E.M. (pc cm^{-6})	3.1 × 10^3	1.1 × 10^6	1.2 × 10^6
	N_e (cm^{-3})	2.13	273	587
RCW 122	T_e (K)	6026	5200	5770
	E.M. (pc cm^{-6})	2.81 × 10^3	9.8 × 10^5	1.2 × 10^6
	N_e (cm^{-3})	6.67	721	1020
RCW 38	T_e (K)	8000	7900	....
	E.M. (pc cm^{-6})	1.13 × 10^4	7.1 × 10^6	4.7 × 10^6
	N_e (cm^{-3})	24.92	4106	2576

a. Obtained from our H166α observations and those of H109α and H76α made by other authors (Wilson *et al.* 1970; McGee and Newton 1981).

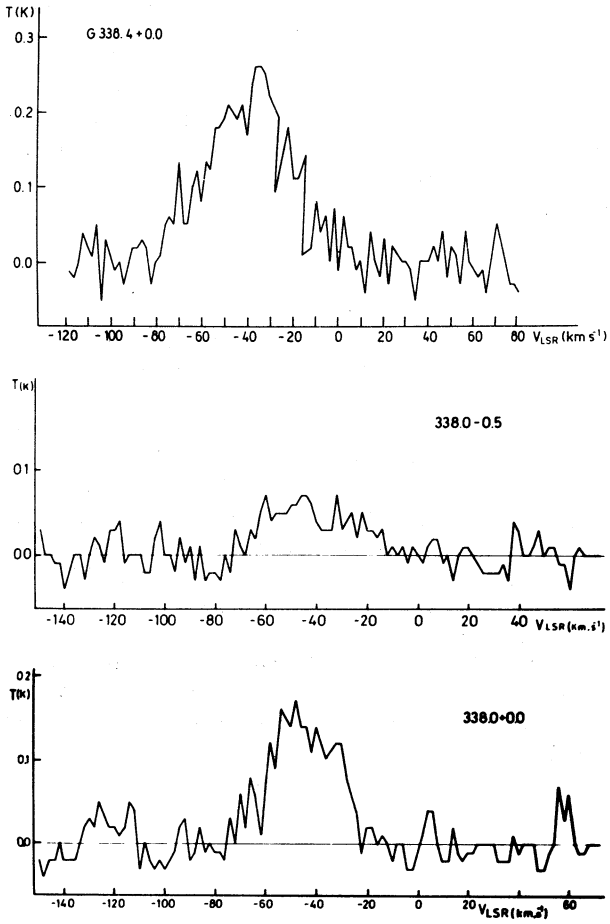

Fig. 3. Some H166α line profiles in the G 338.4+0.0 region.

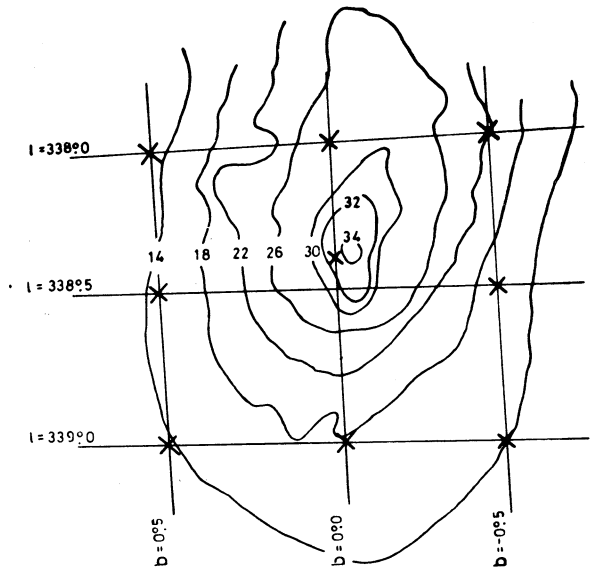

Fig. 4. Continuum map at 1420 MHz of the region associated with G 338.4+0.0. The crosses indicate the positions where the line was observed.

c) *G 331.5–0.1*

Some of our H166α profiles are shown in Figure 5. The central velocities of the profiles are $\simeq -60$ km s^{-1}, with a FWHM ranging from 20 to 30 km s^{-1}.

The continuum map at 1420 MHz of the extended region associated with G 331.5–0.1 with an angular diameter of 100′ is shown in Figure 6. The flux density in the continuum corresponding to this region is $\simeq$ 403 Jy. The average electron temperature is $T_e \simeq$ 5750 K. By using the simplified model of Schraml and Mezger (1969), we obtained values for the electron density, $N_e \simeq 2.76$ cm^{-3} and an emission measure E.M. $\simeq 3.58 \times 10^3$ pc cm^{-6}. The adopted distance is 11 kpc, which yields a diameter of the region of D = 320 pc. The results obtained from higher frequency recombination line observations (Wilson *et al.* 1970), (Mc Gee and Newton 1981), give values for the elctron density and the emission measure by 2 or 3 orders of magnitude higher than those obtained from H166α observations (see Table 1).

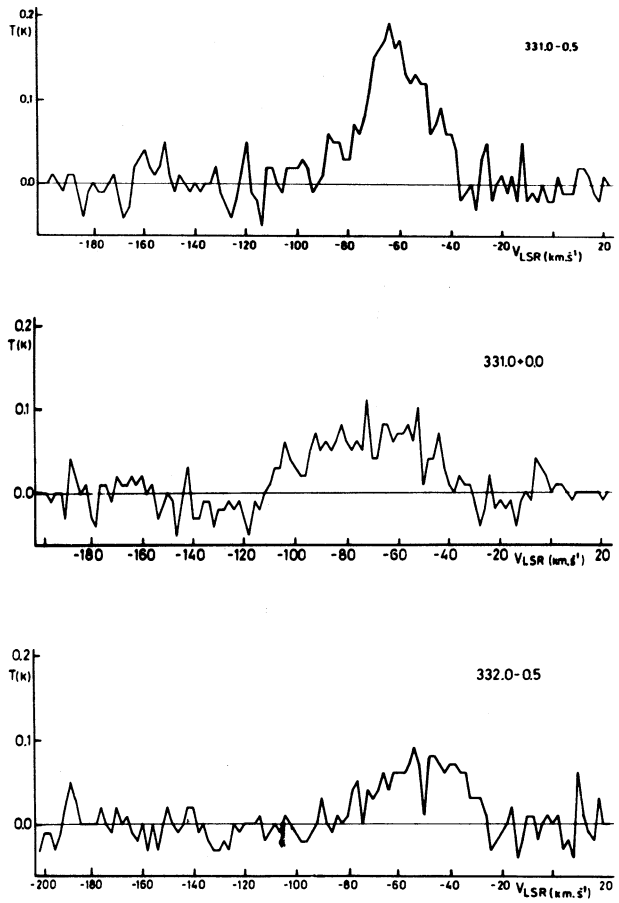

Fig. 5. Some H166α profiles obtained in the G 331.5–0.1 region.

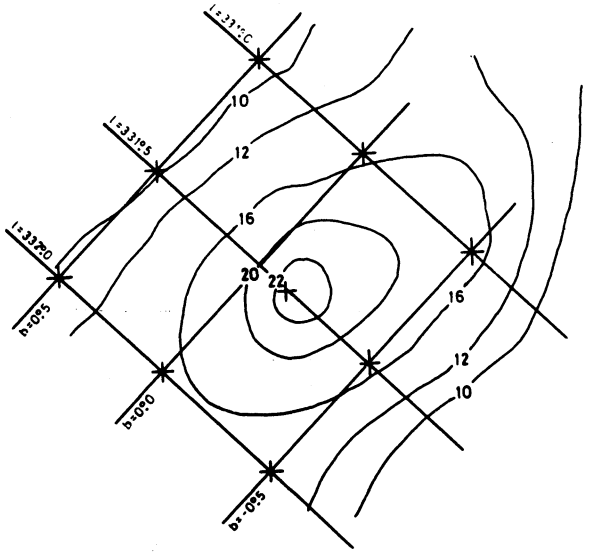

Fig. 6. Continuum map at 1420 MHz of the region associated with G 331.5−0.1. The crosses indicate the positions where the H166α line was observed.

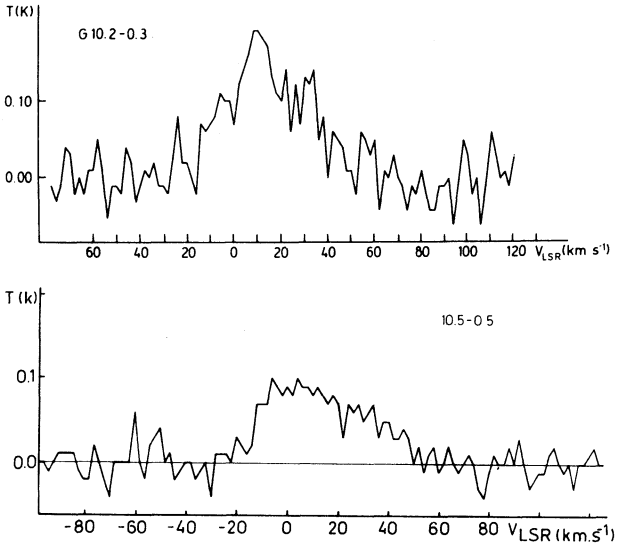

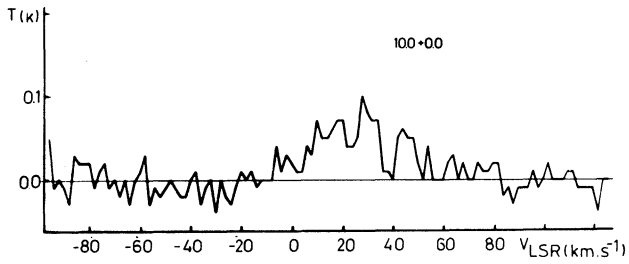

Fig. 7. Some H166α profiles in the W 31 region.

d) *W 31*

Some of the H166α profiles obtained from the extended region associated with W 31 (whose center has galactic coordinates l = 10°.2, b = −0°.3) are shown in Figure 7. The centroid velocities of the profiles are ≃ 12 km s^{-1}, with a FWHM ≃ 46 km s^{-1}. The continuum map of the region at 1420 MHz is shown in Figure 8. The positions where the H166α line was observed are indicated by crosses.

The continuum flux density corresponding to the extended region of angular diameter 93′, is 306 Jy. The corresponding electron temperature is ≃ 5600 K. The adopted distance is 17.2 kpc yielding a diameter of D ≃ 465 pc. By using the same simplified model as that used for the previous regions, we obtained values for the density, N_e ≃ 2.13 cm^{-3} and emission measure E.M. ≃ 3.1 × 10^3 pc cm^{-6}.

Again the values for electron density and emission measure obtained from higher frequencies recombination line observations (Wilson *et al.* 1970; Mc Gee and Newton 1981) are 2 or 3 orders of magnitude larger than those obtained by us from the H166α observations. The same explanations given for the previous H II regions are also valid here.

e) *RCW 122*

Some of the profiles obtained in H166α are shown in Figure 9. The central velocities of the profiles are ≃ −40 km s^{-1}, with a FWHM of ≃ 36 km s^{-1}.

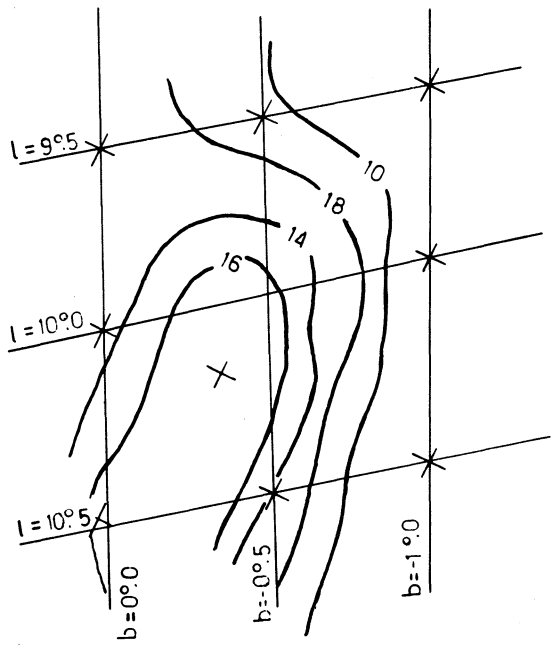

Fig. 8. Continuum map at 1420 MHz of the region associated with W 31. The crosses indicate the positions where the line was observed.

The continuum map at 1420 MHz of the associated region with an angular diameter of 74′ is shown in Figure 10. The positions where the H166α line was observed are indicated by crosses. The continuum flux density at 1420 MHz of the extended H II region is $\sim$ 171 Jy. The distance is 2 kpc and the diameter, D = 43 pc. The average electron temperature is $\sim$ 6026 K. Using the very simplified model of Schraml and Mezger (1969), we obtained values for the electron density, $N_e \sim 6.7$ cm^{-3} and for the emission measure, E.M. $\sim 2.81 \times 10^3$ pc cm^{-6}.

The values of density and emission measure obtained from previous observations in H109α and H76α are about 2 or 3 orders of magnitude larger than our values. The same explanation given for the previous regions is also valid here.

f) *RCW 38*

The H166α profile of the central point of the H II region is shown in Figure 11. The continuum map at 1420 MHz of the associated extended region is shown is Figure 12. The observed point is shown by a cross. The distance of the region is 0.6 kpc and the diameter, D $\sim$ 12.4 pc.

The continuum flux density corresponding to the region with an angular diameter of 71′ is $\sim$ 568.5 Jy and the resulting electron temperature is 8000 K. By using the same simplified model of Schraml and Mezger, we obtained 24.9 cm^{-3} for the electron density and an emission measure E.M. $\sim 1.13 \times 10^4$ pc cm^{-6}. The values for these physical parameters obtained from the H109α observations of Wilson *et al.* (1970) and H76α observations of Mc Gee and Newton (1981) are about one order of magnitude larger than our H166α values (see Table 1).

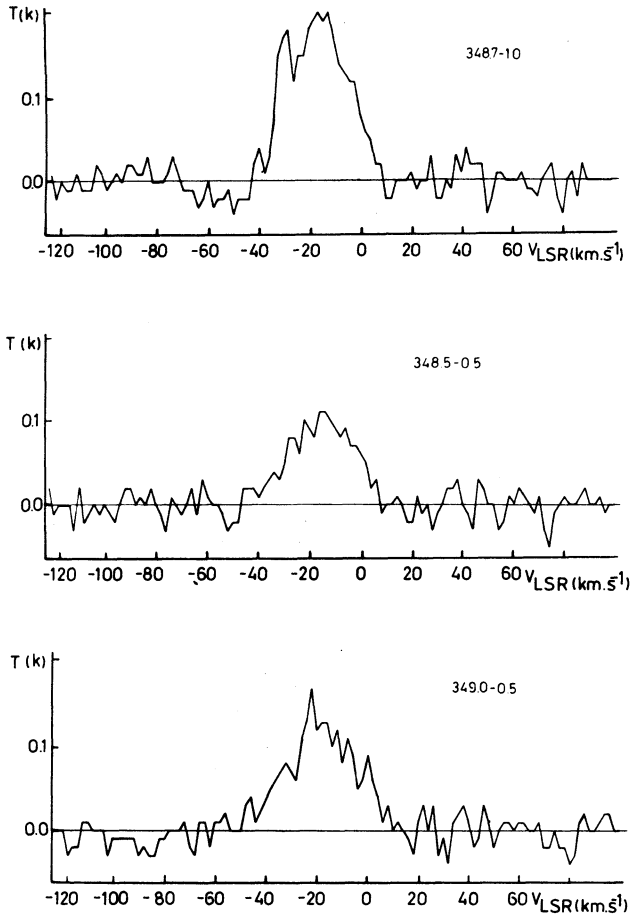

Fig. 9. Some H166α profiles in the RCW 122 region.

TABLE 2

LINE PARAMETERS OF THE PROFILES IN THE BIRGHTEST POSITIONS IN EACH REGION

Source	l (°)	b (°)	T_L (K)	FWHM (km s^{-1})
RCW 49	284.3	− 0.3	0.35	35
G331.5 − 0.1	331.5	− 0.1	0.25	24
G338.4 + 0.0	338.4	− 0.0	0.26	35
W 31	10.2	− 0.3	0.19	45
RCW 122	348.7	− 1.0	0.19	35
RCW 38	268.0	− 1.1	0.23	40

a. T_L is the peak line temperature, l, b and the FWHM have the usual meaning.

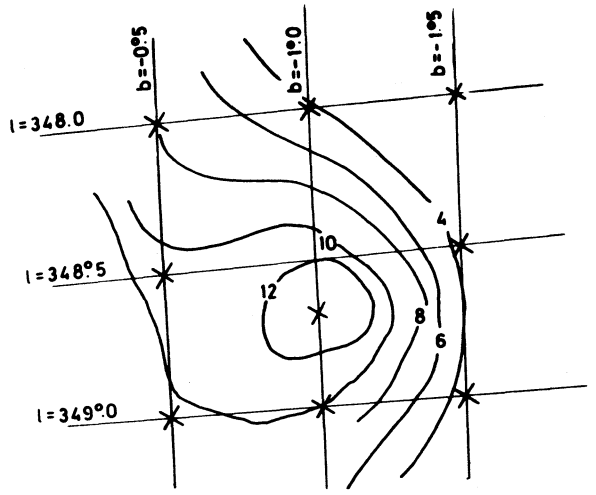

Fig. 10. Continuum map at 1420 MHz of the region associated with RCW 122. The crosses indicate the positions where the line was observed.

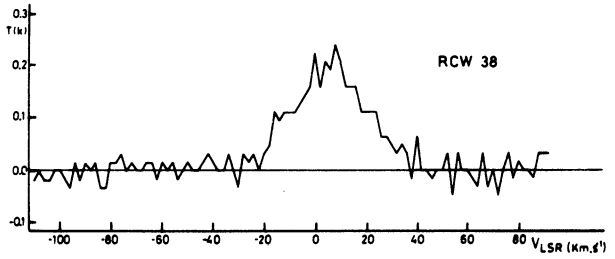

Fig. 11. The H166α profile of the central point of the RCW 38 region.

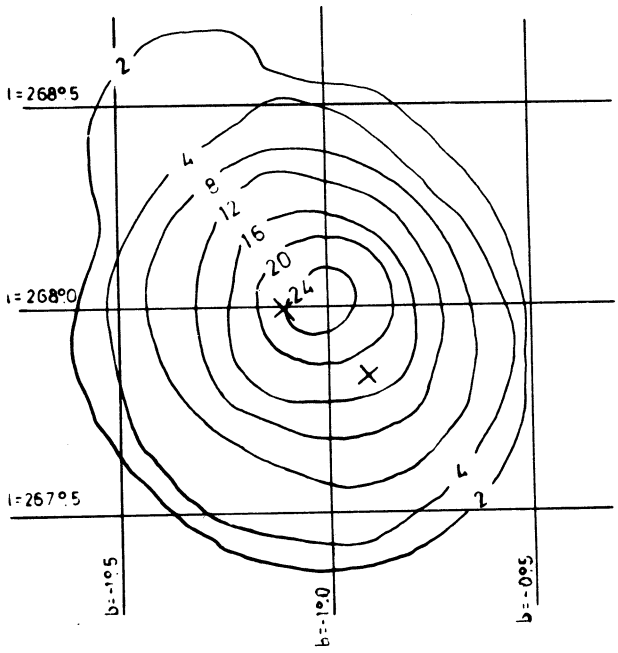

Fig. 12. The continuum map at 1420 MHz of the extended region associated with RCW 38. The crosses indicate the position where the line was observed.

The previous explanation given for the other regions is also valid here.

IV. THERMODYNAMICAL EQUILIBRIUM

In high emission measure regions, there are important departures from LTE at the frequency of 1.4 GHz. This results in an increase of recombination line temperatures, and, therefore generally there is an underestimation of the T_e^*(LTE) (where T_e^* is $\leqslant$ minor or equal). However, for the low density ionized gas ($N_e \backsim 1-10$ cm^{-3}) of low emission measure, the T_e^* obtained from H166α and 1.4 GHz continuum observations, should differ from the actual temperature T_e by less than 20%(Dyson 1969).

In the six regions we observed, the possibility that departures from LTE be present, was investigated through the expression:

$$\frac{T_e}{T_e^*} = \left[b_n \left(1 + \frac{\tau_c}{2} \frac{k\,T_e}{h\nu} \frac{d\ell_n\, b_n}{d\, b_n} \Delta_n \right) \right]^{0.87} \qquad (1)$$

where τ_c is the optical depth for continuum radiation, b_n is the population departure for the atomic level n, k is Boltzmann's constant, h is Planck's constant and ν is the frequency. We obtained values of $T_e/T_e^* \leqslant 1.2$ for the six nebulae, as expected. Because the $\Delta\nu_S/\Delta\nu_D$ ratio (Griem 1967) is unimportant for n > 150 when the density $N_e \leqslant 10^3$ cm^{-3}, pressure broadening does not play a dominant role. $\Delta\nu_S$ is the Stark broadened half-power line width, and $\Delta\nu_D$ is the Doppler half-power width. Then the explanation for the low values of T_e/T_e^* is that departures from LTE are negligible in these observations. We can conclude that the assumption of LTE is a reasonably good approximation for the low density ionized gas associated with the six nebulae.

V. COMMENTS

The extensive observations of the H166α line and 1.4 GHz continuum observations of the six H II regions allowed us to know the values of density and emission measure for the low density gas associated to the regions.

From Table 1, it follows that the observations of higher frequency radio recombination lines, can supply the physical parameters corresponding to the denser gas close to the center of the nebulae.

The combined results (at high and low frequencies) are compatible with the description of the relatively extended H II regions as consisting roughly of a small compact region of gas embedded in an extended ionized gas envelope of lower density. This is also shown in earlier papers (Cersosimo 1982; Azcárate *et al.* 1986, 1987).

However, at least for the H II regions studied in this paper, it would be rather difficult to assess if we are dealing with a core-halo situation or if the density decreases more continuously, since we do not have available observations with several beam sizes.

We wish to thank the technical staff of the Instituto Argentino de Radioastronomía. We are grateful to Mr. J.

Mazzaro for his assistance during the observations, and Mr. M. Campi for making the drawings. We also thank the referee, for useful suggestions to improve the paper.

REFERENCES

Azcárate, I.N., Cersosimo, J.C., and Colomb, F.R. 1986, *Rev. Mexicana Astron. Astrof.*, **13**, 15.
Azcárate, I.N., Cersosimo, J.C., and Colomb, F.R. 1987, *Rev. Mexicana Astron. Astrof.*, **15**, 3.
Caswell, J.L. and Robinson, B.J. 1974, *Australian J. Phys.*, **27**, 597.
Cersosimo, J.C. 1982, *Ap. J. (Letters)*, **22**, 157.
Cersosimo, J.C. 1985, *Rev. Mexicana Astron. Astrof.*, **10**, 171.
Dyson, J.E. 1969, *Ap. and Space Sci.*, **4**, 401.
Gillespie, A.R. *et al.* 1977, *Astr. and Ap.*, **60**, 221.
Griem, H.R. 1967, *Ap. J.*, **148**, 157.
Mc Gee, R.X., Newton, L.M., and Batchelor, R.A. 1975, *Australian J. Phys.*, **28**, 185.
Mc Gee, R.X. and Newton, L.M. 1981, *M.N.R.A.S.*, **196**, 889.
Schraml, J. and Mezger, P.G. 1969, *Ap. J.*, **156**, 269.
Whiteoak, J.B. and Gardner, F.F. 1974, *Astr. and Ap.*, **37**, 389.
Whiteoak, J.B. and Gardner, F.F. 1979, *M.N.R.A.S.*, **185**, 33p.
Wilson, T.L., Mezger, P.G., Gardner, F.F., and Milne, D.K. 1970, *Astr. and Ap.*, **6**, 364.

I.N. Azcárate, J.C. Cersosimo, and F.R. Colomb: Instituto Argentino de Radioastronomía, Casilla de Correo No. 5, (1894) Villa Elisa, Prov. de Buenos Aires, Argentina.